

## Cellular Biophysics During Freezing of Rat and Mouse Sperm Predicts Post-thaw Motility<sup>1</sup>

Mie Hagiwara,<sup>5</sup> Jeung Hwan Choi,<sup>5</sup> Ramachandra V. Devireddy,<sup>9</sup> Kenneth P. Roberts,<sup>4,7,8</sup> Willem F. Wolkers,<sup>3,5</sup> Antoine Makhoul,<sup>7</sup> and John C. Bischof<sup>2,5,6,7</sup>

Departments of Mechanical Engineering,<sup>5</sup> Biomedical Engineering,<sup>6</sup> Urologic Surgery,<sup>7</sup> and Integrative Biology & Physiology,<sup>8</sup> University of Minnesota, Minneapolis, Minnesota  
Department of Mechanical Engineering,<sup>9</sup> Louisiana State University, Baton Rouge, Louisiana

### ABSTRACT

Though cryopreservation of mouse sperm yields good survival and motility after thawing, cryopreservation of rat sperm remains a challenge. This study was designed to evaluate the biophysics (membrane permeability) of rat in comparison to mouse to better understand the cooling rate response that contributes to cryopreservation success or failure in these two sperm types. In order to extract subzero membrane hydraulic permeability in the presence of ice, a differential scanning calorimeter (DSC) method was used. By analyzing rat and mouse sperm frozen at 5°C/min and 20°C/min, heat release signatures characteristic of each sperm type were obtained and correlated to cellular dehydration. The dehydration response was then fit to a model of cellular water transport (dehydration) by adjusting cell-specific biophysical (membrane hydraulic permeability) parameters  $L_{pg}$  and  $E_{Lp}$ . A “combined fit” (to 5°C/min and 20°C/min data) for rat sperm in Biggers-Whitten-Whittingham media yielded  $L_{pg} = 0.007 \mu\text{m min}^{-1} \text{atm}^{-1}$  and  $E_{Lp} = 17.8 \text{ kcal/mol}$ , and in egg yolk cryopreservation media yielded  $L_{pg} = 0.005 \mu\text{m min}^{-1} \text{atm}^{-1}$  and  $E_{Lp} = 14.3 \text{ kcal/mol}$ . These parameters, especially the activation energy, were found to be lower than previously published parameters for mouse sperm. In addition, the biophysical responses in mouse and rat sperm were shown to depend on the constituents of the cryopreservation media, in particular egg yolk and glycerol. Using these parameters, optimal cooling rates for cryopreservation were predicted for each sperm based on a criteria of 5%–15% normalized cell water at  $-30^\circ\text{C}$  during freezing in cryopreservation media. These predicted rates range from 53°C/min to 70°C/min and from 28°C/min to 36°C/min in rat and mouse, respectively. These predictions were validated by comparison to experimentally determined cryopreservation outcomes, in this case based on motility. Maximum motility was obtained with freezing rates between 50°C/min and 80°C/min for rat and at 20°C/min with a sharp drop at 50°C/min for

mouse. In summary, DSC experiments on mouse and rat sperm yielded a difference in membrane permeability parameters in the two sperm types that, when implemented in a biophysical model of water transport, reasonably predict different optimal cooling rate outcomes for each sperm after cryopreservation.

*cryopreservation, DSC, motility, mouse sperm, rat sperm*

### INTRODUCTION

Mice and rats are the animal models used in about 97% of biomedical research [1]. Although mice and rats are relatively easy to house and breed, it is expensive to maintain and transport transgenic or genetically modified strains [2]. Breeding can also lead to naturally occurring genetic mutations [3]. Cryopreservation of sperm is one solution used in a variety of species to facilitate long-term storage and transportation, thereby reducing the cost of maintaining rodent strains [4, 5]. Cryopreservation of sperm is routinely used for some species. For example, human sperm is cryopreserved for in vitro fertilization and storage using glycerol and egg yolk media as cryoprotective agents (CPAs) [4]. In the breeding of domestic animals and cattle, where artificial insemination (AI) is extensively used, cryopreservation in glycerol-based media facilitates transport of semen [6, 7]. The maintenance of many mouse sperm lines is achieved by cryopreservation, predominantly using raffinose and skim milk as CPAs [2, 8, 9]. Despite successful sperm cryopreservation of some species, for many others cryopreservation remains a challenge [10].

One important rodent model that remains difficult to cryopreserve is the rat. Rats are a preferred model over mice for many studies because of their larger size [11]. Therefore, there continues to be a strong interest in developing a method to cryopreserve rat sperm successfully. Only one group has reported successful cryopreservation of rat sperm, subsequently used for AI and yielding live offspring [12, 13]. This result has not yet been repeated by other investigators or labs, and further investigation of the ability to yield viable rat sperm after cryopreservation is urgently needed [10]. This work examines the cellular biophysics that occurs during rat sperm cryopreservation and compares these results to those of a successfully cryopreserved rodent species, the mouse. The goal of this study is to determine if there are underlying differences in the biophysical mechanisms of water transport (dehydration) and injury that differentiate these two species' sperm and to suggest improved approaches for rat sperm cryopreservation.

Biophysical responses in cells during freezing have been studied extensively, although challenges exist for sperm due to their size and nonspherical shape. When cells are cooled in suspension, ice nucleates first in the extracellular space, leading to the biophysical responses of cellular dehydration and/or

<sup>1</sup>Supported by the National Institutes of Health (NIH) grant R21 RR021698-01 and by the Institute for Engineering in Medicine at the University of Minnesota.

<sup>2</sup>Correspondence: John C. Bischof, Department of Mechanical Engineering, University of Minnesota, 111 Church St. SE, Minneapolis, MN 55455. FAX: 612 625 4344; e-mail: bischof@umn.edu

<sup>3</sup>Current address: Institut für Mehrphasenprozesse, Leibniz Universität Hannover, Hannover, Germany.

<sup>4</sup>Current address: WWAMI Medical Education Program, Washington State University-Spokane, Spokane, WA.

Received: 7 January 2009.

First decision: 14 March 2009.

Accepted: 28 May 2009.

© 2009 by the Society for the Study of Reproduction, Inc.

eISSN: 1259-7268 <http://www.biolreprod.org>

ISSN: 0006-3363

intracellular ice formation (IIF). Both extreme dehydration at slow cooling rates and large, stable IIF at fast cooling rates can destroy cells. However, optimal survival can be obtained at intermediate cooling rates that minimize both of these injury mechanisms, as has been demonstrated for a variety of cells [14–16]. Optimal cooling rates that yield the highest post-thaw survival can be predicted based on experimentally determined, cell-specific parameters, including the membrane hydraulic permeability,  $L_p$  (which is dependent upon parameters  $E_{Lp}$  and  $L_{pg}$  and is further described in *Materials and Methods*), and heterogeneous ice nucleation parameters [17]. The relationship of these parameters to the biological response of cells has been explained previously [10, 18]. Experimental techniques to determine cell-specific membrane hydraulic permeability parameters ( $E_{Lp}$  and  $L_{pg}$ ) during freezing traditionally rely on optical cryomicroscopy, which works well for larger spherical cells where two-dimensional cell areas can be extrapolated to three-dimensional cell volumes. However, this technique does not work for sperm, which are nonspherical and too small. Thus, new approaches to measure sperm biophysical responses during freezing are needed.

Several techniques are available to measure the biophysics of sperm. However, only the differential scanning calorimeter (DSC) technique allows measurement of subzero dehydration behavior in the presence of ice and CPAs to be tested [19]. Previous work on sperm has shown that membrane hydraulic permeability values from DSC (ice present) are much smaller than permeability values obtained with suprazero techniques (ice absent) [10, 19]. Recent work suggests the reduction in membrane permeability in the presence of ice is due to extreme lipid or membrane packing (i.e., creation of a gel phase), a mechanism absent at suprazero temperatures [20]. The DSC measures excess latent heat due to cellular dehydration in the presence of ice in sperm and other cell types during a specific cooling rate protocol [19, 21, 22]. This dehydration response can be used to extract the membrane hydraulic permeability,  $L_{pg}$ , and the corresponding activation energy,  $E_{Lp}$ , for rat and mouse sperm. Using these parameters, water transport can be simulated during freezing, and optimal cooling rates for cryopreservation can be predicted. The predicted optimal cooling rates can be separately verified for both rat and mouse by assessing cryopreservation outcomes, in this case by motility measurements. The present work uses DSC to reveal differences in freezing biophysics between rat and mouse sperm that help explain differences in cryopreservation outcome between these two rodent sperm types.

## MATERIALS AND METHODS

All procedures described within were reviewed and approved by the University of Minnesota Institutional Animal Care and Use Committee and were performed in accordance with the Guiding Principles for the Care and Use of Laboratory Animals.

### Sperm Collection and Handling

*Rat.* Caudal sperm of Hsd:SD:Hsd proven breeder rats (Harlan, Indianapolis, IN) were collected. This species was chosen because it was readily available and inexpensive. A pair of cauda epididymides was excised from a rat. Several small incisions were made to allow sperm to elute into 1 ml of elution buffer for 5 min at 37°C. Two elution buffers were used for rat sperm DSC study: modified Biggers-Whitten-Whittingham (mBWW) [23] and a cryopreservation media containing 23% (v/v) egg yolk, 8% (w/v) lactose monohydrate, and antibiotics (described by Nakatsukasa [12] as media I). For samples to be used in DSC measurements, the eluted sperm were centrifuged for 5 min at 700 × g. The supernatant was removed, and the remaining sample size was 0.2 ~ 0.5 ml. For freeze-thaw experiments and motility assessments, rat sperm were cryopreserved according to the method of Nakatsukasa et al. [12], the only method to date used to successfully cryopreserve rat sperm.

Briefly, rat sperm were eluted into Nakatsukasa media I but did not undergo a centrifugation step. Following elution in Nakatsukasa media I, the sperm were cooled and maintained at 15°C for 30 min and then at 5°C for 30 min. Following the second cooling step, an equal volume of Nakatsukasa media II, containing media I + 1.4% (v/v) Equex Stem (Nova Chemical Sales, Inc., Scituate, MA), was added. This final cryoprotective medium is referred to as Nakatsukasa media III (521 mOsm total, 224 mM lactose) [12]. Rat sperm motilities were assessed before and after freeze-thaw (see *Cryopreservation Outcome (Motility after Freeze-Thaw)*).

*Mouse.* Caudal sperm of Hsd:ICR (CD-1) retired breeder mice (Harlan) were collected by excision from two mice. For DSC study, Dulbecco phosphate-buffered saline solution (D-PBS [pH 7.2]; Life Technologies, Grand Island, NY) was used as elution buffer. For samples to be used in DSC measurements, the eluted sperm were centrifuged for 5 min at 300 × g. The result was compared to previously published data using D-PBS with 15% egg yolk as well as to the low CPA media of D-PBS containing 15% egg yolk, 0.135 M glycerol, and 0.13 M raffinose, described in Devireddy [19]. For freeze-thaw experiments and motility assessments, mouse sperm were eluted into the 15% egg yolk in D-PBS elution buffer, and CPA was added stepwise to a final concentration of 0.135 M glycerol and 0.13 M raffinose, described in Devireddy [19]. The samples did not undergo a centrifugation step for freeze-thaw experiments and motility assessments. Mouse sperm motilities were assessed before and after freeze-thaw (see *Cryopreservation Outcome (Motility after Freeze-Thaw)*).

### DSC Studies

A DSC dynamic cooling program was used to measure water transport out of rat and mouse sperm cells as previously described [19]. Briefly, sperm samples were placed in standard aluminum sample pans (Perkin Elmer Life and Analytical Sciences, Inc., Waltham, MA) with <0.1 mg powdered *Pseudomonas syringae* (Snomax, York International, CO). The samples were nucleated by cooling to -5°C and then rewarmed to a temperature slightly below the melting point ( $T_m$ ) so that small amounts of ice crystals remain. The samples were then exposed to 5°C/min or 20°C/min cooling rates until a temperature of -30°C was reached. Subsequently, the cells were lysed by performing a rapid freeze to -150°C, then the cooling step from  $\sim T_m$  to -30°C was repeated with the now-lysed cells. Figure 1 shows the heat-release thermogram for the initial and final cooling steps. The difference in total area under the curve  $\Delta q_{total} = q_{initial} - q_{final}$ , represented by the shaded area, is a measure of the water transport out of the cells [24] and is used to calculate the volumetric change as shown in Equation 1:

$$\frac{V(T) - V_b}{V_o - V_b} = \frac{\Delta q(T)}{\Delta q_{total}}, \quad (1)$$

where  $V(T)$  is the cell volume at temperature  $T$ ,  $V_b$  is the osmotically inactive cell volume,  $V_o$  is the isotonic cell volume, and  $\Delta q(T)$  is the accumulated partial area of  $\Delta q_{total}$  evaluated at temperature  $T$ . For example, in Figure 1,  $\Delta q(T)/\Delta q_{total}$  would be 0 at  $T = -0.53^\circ\text{C}$  and 1 at  $T = -12^\circ\text{C}$ . It should be noted that Equation 1 is based on an assumption that the cell exists in an isotonic medium prior to freezing, so  $V_o$  needs to be replaced by  $V_i$ , the actual initial volume prior to freezing, if it is placed in a nonisotonic medium.

The measured difference in heat release for rat sperm in mBWW ranged from 5.9 to 13.1 mJ/mg, which is similar to previous work (9–11 mJ/mg for mouse sperm [19]). This is within the range expected, given the cell concentration of the sample (~100 million/ml) and the estimated volume of osmotically active water in the sperm.

### Prediction of Cellular Biophysics: A Model for Water Transport During Freezing

A previously developed mathematical model [25–28] was used to simulate the water transport of sperm cells during freezing as follows:

$$\frac{dV}{dT} = -\frac{L_p A_c}{B} (\Delta\pi) \quad (2)$$

where,  $V$  is the sperm cell volume ( $\mu\text{m}^3$ ) at temperature  $T$  (K),  $A_c$  is the effective membrane surface area for water transport ( $\mu\text{m}^2$ ), which is assumed to be constant during the freezing process,  $\Delta\pi$  is the difference in osmotic pressure between the intracellular and extracellular compartment,  $B$  is cooling rate (K/min), and  $L_p$  is the membrane hydraulic permeability to water defined by Levin [27] as

$$L_p = L_{pg} \exp\left(-\frac{E_{Lp}}{R} \left(\frac{1}{T} - \frac{1}{T_R}\right)\right), \quad (3)$$

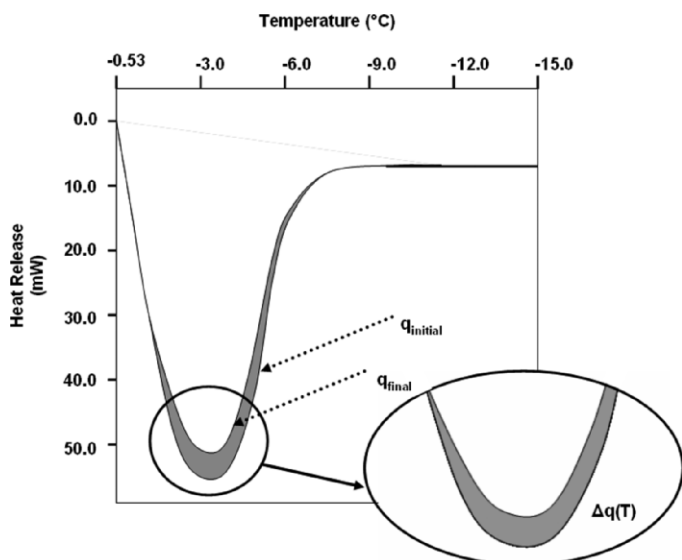


FIG. 1. The heat flow versus temperature curves for DSC measurement. The lower and upper curves correspond to the heat release measured for the live osmotically active and lysed osmotically inactive cells, respectively. The difference between the initial and final heat flows ( $\Delta q$ ) is the measure of osmotically active water during sperm dehydration in the system.

where  $T_R$  is the reference temperature (273.15 K),  $L_{pg}$  is the membrane hydraulic permeability at  $T_R$  ( $\mu\text{m min}^{-1} \text{atm}^{-1}$ ),  $E_{Lp}$  is the activation energy for water transport (kcal/mol), and  $R$  is the universal gas constant ( $8.314 \text{ J mol}^{-1} \text{K}^{-1}$ ).

In this study, the sperm cells are modeled as long cylinders. The sperm cells are modeled using a length of  $188.7 \mu\text{m}$  and a diameter of  $1.42 \mu\text{m}$  for rat, and a length of  $122 \mu\text{m}$  and a diameter  $0.92 \mu\text{m}$  for mouse. These geometric parameters were taken from Devireddy et al. [19] and Cummins and Woodall [29]. The osmotically inactive cell volume,  $V_{ip}$ , was assumed to be the same as for mouse sperm ( $0.61V_o$ ), as reported by Willoughby et al. [30]. The membrane permeability parameters ( $L_{pg}$  and  $E_{Lp}$ ) were determined by selecting values that would bring about a best fit of the volumetric change based on Equation 2, with the volumetric change measured using the DSC.

The best-fit parameters were then used for simulation of rat and mouse sperm biophysical responses, with adjustment of initial osmolality due to media (rat in media III) and ice-seeding temperature ( $-3^\circ\text{C}$ ). Optimal rates of cooling were defined as those that leave between 5%–15% of the initially active water trapped inside the cells at  $-30^\circ\text{C}$ . This condition is based on the premise that optimal survival will be obtained by minimizing dehydration or solution effects injury during slow cooling (such that at least 5% of water remains) and by minimizing IIF during fast cooling (so that less than 15% of the water changes to ice within the cell). This approach has been presented in numerous studies [14, 15, 18, 19].

### Cryopreservation Outcome (Motility After Freeze-Thaw)

Motility was measured in rat and mouse sperm as an indirect measure of sperm viability prefreeze and post-thaw. We have shown that motility is comparable to dye exclusion assays for measurement of mouse sperm viability [19]. Our own experience and the data in the literature suggest that dye exclusion assays underestimate viability in rat sperm [12, 31]. Control rat sperm motility (progressive) measured using computer-assisted semen analysis (CASA) was  $63\% \pm 10\%$  in mBWW. However, progressive motility was reduced to zero in freezing medium, though a high percentage of sperm remained nonprogressively motile (twitching) when assessed visually using a microscope, indicating that many sperm were still viable. Twitching is often used as a measure of sperm viability in the clinical setting when selecting a human sperm for ICSI [32, 33]. Upon dilution of the rat sperm out of the freezing medium and into mBWW, progressive motility returned to  $18\% \pm 8\%$ , indicating that manipulating sperm into and out of freezing medium injures the cells, as measured by progressive motility. A freeze-thaw step after introduction into the freezing medium reduced the progressive motility to essentially 0% upon dilution into mBWW. Therefore, it was clear that both freeze-thaw and handling contributed to the loss of progressive motility in rat

sperm. As a result, we elected to measure nonprogressive sperm motility directly after freeze-thaw by direct observation using a light microscope while the rat sperm were still within the freezing medium. This technique appeared to be the best possible approach for yielding new information on the survival of rat sperm directly after freeze-thaw.

Both rat and mouse sperm samples of  $150 \mu\text{l}$ , prepared as described below, were frozen on the Linkam cryostage (Linkam BCS196 Cryobiology System, Surrey, U.K.) in a circular quartz crucible. Samples were frozen at various cooling rates ranging from  $2^\circ\text{C/min}$  to  $130^\circ\text{C/min}$ , with an end temperature of  $-80^\circ\text{C}$ . The samples were then rewarmed to room temperature at  $130^\circ\text{C/min}$ , and motility was assessed as noted below.

**Rat.** Rat sperm samples in media III (or mBWW negative control) were nucleated with a chilled needle at  $-3^\circ\text{C}$  and then frozen to an end temperature of  $-80^\circ\text{C}$  at various cooling rates. As discussed above, nonprogressive motility was determined as a measure of rat sperm viability. Briefly, a light microscope (Olympus BH2 light microscope, Tokyo, Japan) at  $20\times$  was used both before and after freezing to visually assess nonprogressive motility. A microslide (#HTR 1099; VitroCom Inc., Mountain Lakes, NJ) containing a  $0.1 \times 2.0 \text{ mm}$  cannula was placed directly into the control or frozen-thawed sperm solution. After the sample was loaded into the cannula by capillary action, manual assessments of motility were performed at  $20\times$ . Three hundred sperm per slide were counted. For rat sperm samples in media III, motility was assessed before (control) and after freezing, both with 1:10 dilution in media I at  $37^\circ\text{C}$ . For negative control sperm samples in mBWW, motility was also assessed before and after freezing, but the 1:10 dilution was performed using mBWW only. The post-thaw motility was normalized to the prefreeze motility. No motility was found in the negative control of rat sperm frozen in mBWW.

**Mouse.** Mouse sperm ( $150 \mu\text{m}$ ) in low-CPA media (or D-PBS as negative control) were nucleated with a chilled needle at  $-8^\circ\text{C}$  and then warmed to  $-2^\circ\text{C}$  before freezing on the Linkam cryostage to  $-80^\circ\text{C}$  at various cooling rates. This nucleation temperature was necessary to overcome the higher concentration of CPA in mouse cryopreservation media compared to rat media, and was further chosen to match Devireddy et al. [19], in which the nucleation temperatures varied between  $-7.4^\circ\text{C}$  and  $-8.5^\circ\text{C}$  for freeze-thaw study. The samples were cooled to an end temperature of  $-80^\circ\text{C}$  at various cooling rates. The samples were then rewarmed to room temperature at  $130^\circ\text{C/min}$ , and motility was assessed. The initial (control) motility of the samples was assessed after 1:10 dilution with 1% bovine serum albumin/Hepes-buffered saline solution (Life Technologies), as described in [19]. Post-thaw mouse sperm motility was similarly assessed and normalized to the prefreeze motility using the same dilution conditions. Factory-preprogrammed CASA settings for mouse were used to assess motility. Freeze-thaw treated samples ( $10 \mu\text{l}$ ) were transferred to glass slides ( $20 \mu\text{m}$  in depth). The CASA software was set to report the average of 10 readings of different fields per sample. The control was kept at room temperature. Progressive motility of the frozen-thawed sperm was normalized with respect to the unfrozen control. No motility was found after freeze-thaw for the negative control of mouse sperm frozen in D-PBS.

## RESULTS

### DSC Studies on Water Transport During Freezing

Figure 2A shows the rat sperm water-transport data from DSC experiments at  $5^\circ\text{C/min}$  and  $20^\circ\text{C/min}$  in media I. For comparison, Figure 2B shows the DSC water-transport data for mouse sperm in low CPA, published previously [19]. It is noted that the osmolality of the suspending solutions for rat and mouse sperm were different, thereby leading to different initial normalized volumes. The water-transport data for all cases investigated were fit to Equation 2, and the results are summarized in Table 1. The combined best-fit membrane permeability parameters for rat sperm were determined in mBWW as  $L_{pg} = 0.007 \mu\text{m min}^{-1} \text{atm}^{-1}$  and  $E_{Lp} = 17.8 \text{ kcal/mol}$  ( $R^2 = 0.95$ ) and in media I as  $L_{pg} = 0.005 \mu\text{m min}^{-1} \text{atm}^{-1}$  and  $E_{Lp} = 14.3 \text{ kcal/mol}$  ( $R^2 = 0.95$ ). The combined best-fit membrane permeability parameters for mouse sperm were determined in D-PBS as  $L_{pg} = 0.009 \mu\text{m min}^{-1} \text{atm}^{-1}$  and  $E_{Lp} = 21.8 \text{ kcal/mol}$  ( $R^2 = 0.97$ ). Previously reported values in D-PBS and 15% egg yolk and in low-CPA media for mouse sperm are also shown in Table 1 for comparison [19]. The data show that rat sperm in mBWW and egg yolk media have lower  $L_{pg}$  and  $E_{Lp}$  than does mouse sperm.

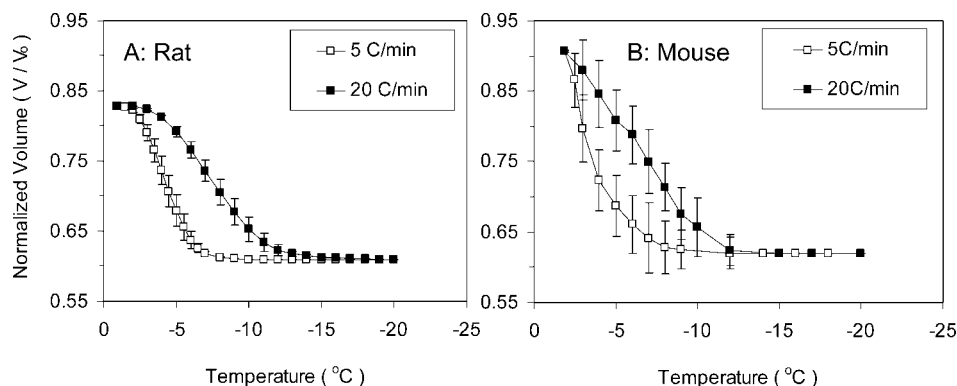


FIG. 2. Volumetric response of rat (A) and mouse (B) sperm cells as a function of subzero temperatures obtained using the DSC technique. Rat sperm were cooled in egg yolk media I and mouse sperm in low-CPA raffinose glycerol media. The filled and unfilled symbols show 20°C/min and 5°C/min data, respectively. Values are given as mean  $\pm$  SD.

### Modeling: Prediction of Cell Dehydration During Freezing

To simulate water transport of sperm under a variety of cooling rates, experimentally obtained values of  $L_{pg}$  and  $E_{LP}$  (Table 1), dimensional parameters (see *Prediction of Cellular Biophysics: A Model for Water Transport During Freezing in Materials and Methods*), and the osmolality of the solution (media III for rat and low CPA for mouse) were taken as input parameters for the water transport Equations 2 and 3. Figure 3 depicts the predicted volumetric response of sperm cells at various cooling rates as a function of subzero temperatures. The predicted optimal cooling rates ( $CR_{opt}$ ) for rat sperm in media III were found to be 53°C/min to 70°C/min (shown as the shaded region). For comparison, previously published membrane permeability parameters and initial conditions were used to predict the optimal cooling rate for mouse in low CPA to be 28°C/min to 36°C/min [18]. Clearly, the optimal rates are lower for mouse than for rat sperm in their respective cryopreservation media.

### Motility/Outcome

Results of rat and mouse sperm post-thaw motility with egg yolk-containing media were normalized to prefreeze controls and are shown in Figure 4. The optimal cooling range from Figure 3 is also shown as the shaded area for comparison. Motility was taken as a measure of cell viability, and cell membrane integrity was then assumed intact if the cell maintained motility. As both plots show, survival versus cooling rate shows the expected inverted U-shaped curve, indicating that the highest motility occurs between the slow

cooling rate, which yields excessive dehydration, and the fast cooling rate, which favors large, stable IIF. Figure 4A shows the normalized motility of post-thaw rat sperm, indicating the peak motility at cooling rates between 50°C/min and 80°C/min. Figure 4B shows that mouse sperm achieved the optimal survival following cryopreservation at 20°C/min, with progressive motility of approximately 30% that drops sharply by 50°C/min. Additionally, negative control freeze-thaw experiments were also performed for both rat and sperm with elution media that did not contain egg yolk, and no progressive motility or twitching was observed after freeze-thaw.

### DISCUSSION

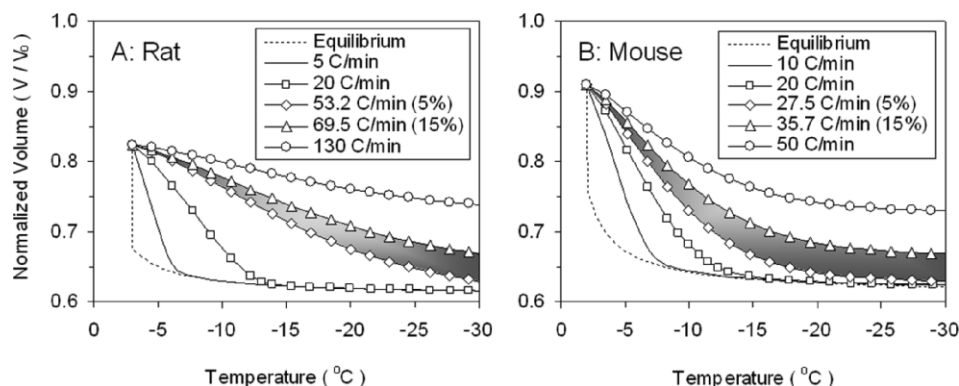
In the current study, differential scanning calorimetry was used as the biophysical measurement technique to study the freezing response of rat and mouse sperm and to yield insight into their differential cryopreservation responses. Other biophysical measurement techniques exist, including time to lysis, Coulter counter, and electron spin resonance/electron paramagnetic resonance approaches [30, 34–39]. All of these measurements are at suprazero temperatures, or in the absence of extracellular ice. Importantly, the DSC technique in sperm has generated membrane permeability parameters that are significantly less than those from suprazero studies mentioned above and recently reviewed [10]. This reduction in membrane hydraulic permeability is due to an increase in activation energy and a reduction in the reference permeability compared to suprazero techniques [19, 22]. We recently published a study describing a correlative technique (Fourier transform infrared spectroscopy—FTIR) that shows that the cell membrane

TABLE 1. Best-fit water transport parameters of rat and mouse sperm determined by DSC and fit by FORTRAN (Formula Translation Computer Language) optimization as previously reported in Devireddy et al. [19].

| Experimental system                 | Cooling rate      | $L_{pg}$ ( $\mu\text{m min}^{-1}\text{atm}^{-1}$ ) | $E_{LP}$ (kcal/mol) | $R^2$ value |
|-------------------------------------|-------------------|--|---------------------|-------------|
| Rat sperm (mBWW)                    | 5°C/min           | 0.008  | 26.4                | 0.98        |
|                                     | 20°C/min          | 0.01   | 20.2                | 0.98        |
|                                     | Combined best fit | 0.007  | 17.8                | 0.95        |
| Rat sperm (Nakatsukasa media I)     | 5°C/min           | 0.005  | 18.2                | 0.97        |
|                                     | 20°C/min          | 0.005  | 11.5                | 0.99        |
|                                     | Combined best fit | 0.005  | 14.3                | 0.97        |
| Mouse sperm (D-PBS)                 | 5°C/min           | 0.01   | 56.5                | 0.99        |
|                                     | 20°C/min          | 0.009  | 20.2                | 0.99        |
|                                     | Combined best fit | 0.009  | 21.8                | 0.97        |
| Mouse sperm (D-PBS + 15% egg yolk)* | 5°C/min           | 0.01   | 50.6                | 0.98        |
|                                     | 20°C/min          | 0.01   | 20.5                | 0.96        |
|                                     | Combined best fit | 0.01   | 22.5                | 0.94        |
| Mouse sperm* (low CPA)              | 5°C/min           | 0.008  | 34.3                | 0.99        |
|                                     | 20°C/min          | 0.009  | 26.9                | 0.99        |
|                                     | Combined best fit | 0.01   | 29.2                | 0.98        |

\* Data from Devireddy et al. [19].

FIG. 3. Predicted response to cooling for rat (A) and mouse (B) sperm. Predictions are based on rat sperm in egg yolk media III and mouse sperm in low-CPA raffinose glycerol media. The model-simulated dynamic cooling response using the combined-fit  $L_{pg}$  and  $E_{Lp}$  values were tested for various cooling rates. The nondimensional volume is plotted along the y-axis and the subzero temperatures are shown along the x-axis. The optimal cooling rate range is shown as the shaded area.



changes dramatically in the presence of extracellular ice. In fact, there is an intense lipid phase change as the membrane enters the gel phase during freezing-induced cellular dehydration that we refer to as “membrane packing” [40]. We further show that the activation energy for lipid (i.e., membrane) packing during freezing in three cell types is comparable to the activation energy for membrane hydraulic permeability during freezing in these same cell types obtained by cryomicroscopy. This not only suggests that the mechanism for a reduction in the permeability (with ice) is membrane packing (i.e., less space for water movement through membrane), but also indicates the necessity of using a subzero technique with ice present in order to accurately measure water transport. Indeed, it is likely that membrane packing in the presence of ice explains the controversy over why dehydration predictions based on suprazero membrane permeability parameters (with no membrane packing) do not match experimentally determined optimal rates for cryopreservation (i.e., optimal rates of cooling with ice present) [10].

At higher cooling rates, one postmortem approach in the presence of ice and CPA uses electron microscopy (EM) techniques to search for ice crystals within the cytoplasm of frozen sperm [41]. The author claims, by EM evaluation of a number of sperm, that no IIF occurs even though dehydration is minimal and that rapidly cooled sperm experience an osmotic shock that injures the membrane upon thawing. This is an interesting, if controversial, result that still does not challenge the well-known inverted U curve survival behavior of sperm with cooling rate. In short, injury to sperm is linked to the dehydration response (or lack of it), which currently can only be measured with DSC in the presence of ice and CPA (egg yolk, raffinose, and/or glycerol) [19, 21, 22].

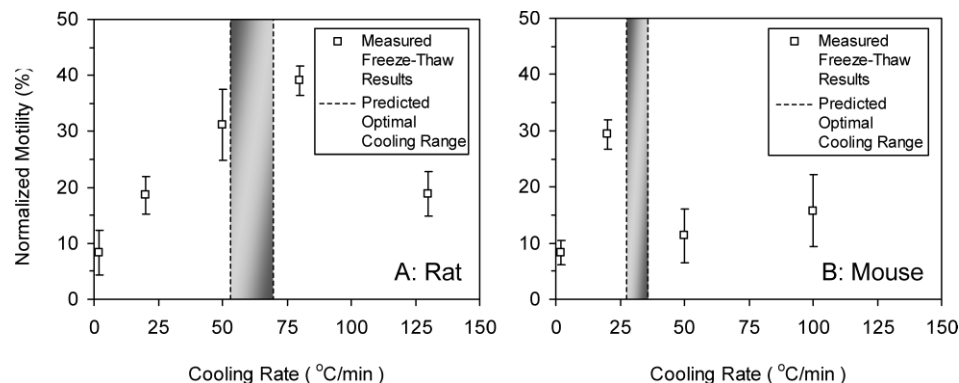
Clear differences were found between the rat and mouse sperm membrane biophysical parameters obtained from these

DSC experiments. In subsequent modeling, these parameters were used to predict different optimal cooling rates for cryopreservation of these sperm. To validate these predictions, motility after freezing was used as a measure of cryopreservation outcome. The results confirm that different rates of cooling are needed for these two sperm types. Specifically, predicted optimal rates for mouse sperm are significantly less (28°C/min to 36°C/min) than for rat (53°C/min to 70°C/min) in their respective cryopreservation media.

DSC results show clear differences in freezing responses at the cellular level between rat and mouse sperm (Fig. 3) and the effect of the suspending media on this freezing response (Table 1). Changes in freezing response are captured in the differences between the “combined fit” biophysical parameters ( $L_{pg}$  and  $E_{Lp}$ ) that are obtained by fitting the DSC measurements as shown here and in previous studies [19]. Using this approach in mouse sperm, we have tested the effect of egg yolk on biophysical measurements. No significant difference was found between mouse sperm samples frozen in D-PBS and in D-PBS with 15% egg yolk. However, previous work with mouse sperm in low-CPA media, which includes 15% egg yolk, 1% glycerol, and 6% raffinose, showed an increase in parameters. This is in contrast to rat sperm, in which significantly higher values of  $L_{pg}$  and  $E_{Lp}$  were found for rat sperm frozen in mBWW vs. media I (23% egg yolk and 8% lactose). It should be noted that though the “combined fit” parameters show the trends as noted, specific fits at 5°C/min and 20°C/min do not necessarily hold this trend. Clearly, these differences in the biophysical parameters in rat vs. mouse with different media require further measurement and understanding. The “combined fit” parameters represent our current best understanding of how these sperm behave in these media during freezing.

The difference in rat and mouse sperm biophysical response may be due to differences in membrane composition and

FIG. 4. Recovered motility of (A) rat and (B) mouse sperm after nucleation and freezing at various rates to  $-80^{\circ}\text{C}$  and thawing at  $130^{\circ}\text{C}/\text{min}$ . Rat sperm were frozen in egg yolk media III and mouse sperm in low-CPA raffinose glycerol media. Values are given as means  $\pm$  SD. The optimal cooling range from Figure 3 is also shown as the shaded area for comparison.



membrane media interactions. It is suggested that the head-group saturation level of the lipid acyl chains and the membrane cholesterol content change membrane fluidity and thus permeability to water. According to Hall et al. [42] and Rejraji et al. [43], the phospholipid fraction of rat sperm membranes is composed of 19.8% phosphatidylcholine (PC) and 28.8% phosphatidylethanolamine (PE), whereas mouse sperm membranes contain 41.4% PC and 18.8% PE. In addition, mouse sperm contain relatively high percentages of polyunsaturated membranous fatty acids compared to rat sperm, and the cholesterol/phospholipid ratio is higher in rat (0.46) than in mouse (0.29) sperm [42, 43]. It is, therefore, not surprising that FTIR studies of several cell types suggest that cell membranes undergo cell-dependent phase changes and lipid alterations during dehydration, and that these events correlate with changes in biophysical response [20, 40].

One approach to predict and explain differences in freezing responses in various cells is through measurement and prediction of biophysical (dehydration) responses. In this study we have measured and used the "combined fit" biophysical parameters in rat and mouse sperm to predict optimal freezing rates for cryopreservation. These predictions were found to compare closely to measured cryopreservation outcomes (in this case motility). The predicted optimal cooling rate in rat sperm based on dehydration is 53°C/min to 70°C/min, which compares well to the experimentally obtained maximum motility results of 50°C/min to 80°C/min. Similarly, in mouse sperm, optimal cooling rates range from 28°C/min to 36°C/min, and the maximum motility is measured at 20°C/min, with an abrupt drop at 50°C/min. It should be noted that DSC and motility experiments were performed under somewhat different cytocrit and nucleation conditions, which may explain the small differences between optimal cooling rate predictions (from DSC measurements) and cryopreservation outcome (from motility).

Although mouse motility is routinely assessed after freeze-thaw in the literature, we are not aware of a routine recovery of motility after freeze-thaw for rat sperm in the literature other than that reported in [12, 13, 31], and thus our data is among the first for rat sperm and the only work to tie motility to biophysical responses. Our studies were not designed to produce optimal results for cryopreservation in either species but rather to study biophysics in a way that rat and mouse sperm can be compared during freezing.

In summary, DSC was used to measure biophysical parameters governing dehydration of rat sperm in media both containing and not containing egg yolk during freezing, and these parameters were compared with behavior in mouse sperm in several media with and without egg yolk and glycerol. Using these biophysical parameters, optimal rates of cryopreservation in both sperm types were predicted and found to match well with optimal cooling rates measured by cryopreservation outcomes (i.e., motility after freeze-thaw). Further studies are needed to reveal the underlying mechanisms (especially the importance of membrane hydration and phase change) that determine the biophysical response of a cell during freezing and how this response is affected by the media. Future work will also need to extend motility results to assessment of fertilizing ability of post-thaw rat sperm under optimal and suboptimal conditions.

## ACKNOWLEDGMENTS

We would like to thank Kathy Bowlin and Laura Piehl for their assistance in preparing the materials and obtaining experimental data. We also would like to acknowledge Raghava Alapati for performing the corroborative DSC experiments at LSU.

## REFERENCES

1. Crawford RL. Information resources on the care and welfare of rodents. AWIC Resource Series [serial online] No. 37. January 9, 2007. Available at: <http://www.nal.usda.gov/awic/pubs/Rodents/rodents.htm>. Accessed July 29, 2009
2. Landel CP. Archiving mouse strains by cryopreservation. *Lab Anim (NY)* 2005; 34:50–57.
3. Buehr M, Hjorth JP, Hansen AK, Sandoe P. Genetically modified laboratory animals—what welfare problems do they face? *J Appl Anim Welf Sci* 2003; 6:319–338.
4. Audrins P, Holden CA, McLachlan RI, Kovacs GT. Semen storage for special purposes at Monash IVF from 1977 to 1997. *Fertil Steril* 1999; 72: 179–181.
5. Woelders H, Matthijs A, Zuidberg CA, Chaveiro AE. Cryopreservation of boar semen: equilibrium freezing in the cryomicroscope and in straws. *Theriogenology* 2005; 63:383–395.
6. Pinkert CA, Dyer TJ, Kooyman DL, Kiehm DJ. Characterization of transgenic livestock production. *Domest Anim Endocrinol* 1990; 7:1–18.
7. Pursel VG, Johnson LA. Freezing of boar spermatozoa: fertilizing capacity with concentrated semen and a new thawing procedure. *J Anim Sci* 1975; 40:99–102.
8. Nakagata N. Cryopreservation of embryos and gametes in mice [in Japanese]. *Jikken Dobutsu* 1994; 43:11–18.
9. Nakagata N. Cryopreservation of mouse spermatozoa. *Mamm Genome* 2000; 11:572–576.
10. Mazur P, Leibo SP, Seidel GE Jr. Cryopreservation of the germplasm of animals used in biological and medical research: importance, impact, status, and future directions. *Biol Reprod* 2008; 78:2–12.
11. Abbott A. Laboratory animals: the renaissance rat. *Nature* 2004; 428:464–466.
12. Nakatsukasa E, Inomata T, Ikeda T, Shino M, Kashiwazaki N. Generation of live rat offspring by intrauterine insemination with epididymal spermatozoa cryopreserved at –196 degrees C. *Reproduction* 2001; 122: 463–467.
13. Nakatsukasa E, Kashiwazaki N, Takizawa A, Shino M, Kitada K, Serikawa T, Hakamata Y, Kobayashi E, Takahashi R, Ueda M, Nakashima T, Nakagata N. Cryopreservation of spermatozoa from closed colonies, and inbred, spontaneous mutant, and transgenic strains of rat. *Comp Med* 2003; 56:511–513.
14. Mazur P. The role of intracellular freezing in the death of cells cooled at supraoptimal rates. *Cryobiology* 1977; 14:251–272.
15. Mazur P. Cryobiology: the freezing of biological systems. *Science* 1970; 168:939–949.
16. Mazur P. Manifestations of injury in yeast cells exposed to subzero temperatures, II: changes in specific gravity and in the concentration and quantity of cell solids. *J Bacteriol* 1961; 82:673–684.
17. Toner M, Cravalho EG, Stachecki J, Fitzgerald T, Tompkins RG, Yarmush ML, Armant DR. Nonequilibrium freezing of one-cell mouse embryos. Membrane integrity and developmental potential. *Biophys J* 1993; 64:1908–1921.
18. Mazur P. Freezing of living cells: mechanisms and implications. *Am J Physiol* 1984; 247:C125–C142.
19. Devireddy RV, Swanlund DJ, Roberts KP, Bischof JC. Subzero water permeability parameters of mouse spermatozoa in the presence of extracellular ice and cryoprotective agents. *Biol Reprod* 1999; 61:764–775.
20. Balasubramanian SK, Wolkers WF, Bischof JC. Membrane hydration correlates to cellular biophysics during freezing in mammalian cells. *Biochimica et Biophysica Acta (BBA). Biomembranes* 2009; 1788:945–953.
21. Devireddy RV, Swanlund DJ, Olin T, Vincente W, Troedsson MH, Bischof JC, Roberts KP. Cryopreservation of equine sperm: optimal cooling rates in the presence and absence of cryoprotective agents determined using differential scanning calorimetry. *Biol Reprod* 2002; 66: 222–231.
22. Devireddy RV, Swanlund DJ, Roberts KP, Pryor JL, Bischof JC. The effect of extracellular ice and cryoprotective agents on the water permeability parameters of human sperm plasma membrane during freezing. *Hum Reprod* 2000; 15:1125–1135.
23. Biggers JP, Whitten WK, Whittingham DG. *The Culture of Mouse Embryos In Vitro*. San Francisco, CA: Freeman; 1971.
24. Devireddy RV, Raha D, Bischof JC. Measurement of water transport during freezing in cell suspensions using a differential scanning calorimeter. *Cryobiology* 1998; 36:124–155.
25. Karlsson JO, Cravalho EG, Borel Rinkes IH, Tompkins RG, Yarmush

- ML, Toner M. Nucleation and growth of ice crystals inside cultured hepatocytes during freezing in the presence of dimethyl sulfoxide. *Biophys J* 1993; 65:2524–2536.
26. Kedem O, Katchalsky A. Thermodynamic analysis of the permeability of biological membranes to non-electrolytes. *Biochim Biophys Acta* 1958; 27:229–246.
27. Levin RL, Cravalho EG, Huggins CE. A membrane model describing the effect of temperature on the water conductivity of erythrocyte membranes at subzero temperatures. *Cryobiology* 1976; 13:415–429.
28. Mazur P. Kinetics of water loss from cells at subzero temperatures and the likelihood of intracellular freezing. *J Gen Physiol* 1963; 47:347–369.
29. Cummins JM, Woodall PF. On mammalian sperm dimensions. *J Reprod Fertil* 1985; 75:153–175.
30. Willoughby CE, Mazur P, Peter AT, Critser JK. Osmotic tolerance limits and properties of murine spermatozoa. *Biol Reprod* 1996; 55:715–727.
31. Yamashiro H, Han YJ, Sugawara A, Tomioka I, Hoshino Y, Sato E. Freezability of rat epididymal sperm induced by raffinose in modified Krebs-Ringer bicarbonate (mKRB) based extender solution. *Cryobiology* 2007; 55:285–294.
32. Stalf T, Mehnert C, Hajimohammad A, Manolopoulos K, Shen Y, Schuppe HC, Diemer T, Schill WB, Weidner W, Tinneberg HR. Influence of motility and vitality in intracytoplasmic sperm injection with ejaculated and testicular sperm. *Andrologia* 2005; 37:125–130.
33. Balaban B, Urman B, Sertac A, Alatas C, Aksoy S, Mercan R, Nuhoglu A. In-vitro culture of spermatozoa induces motility and increases implantation and pregnancy rates after testicular sperm extraction and intracytoplasmic sperm injection. *Hum Reprod* 1999; 14:2808–2811.
34. Noiles EE, Mazur P, Watson PF, Kleinhans FW, Critser JK. Determination of water permeability coefficient for human spermatozoa and its activation energy. *Biol Reprod* 1993; 48:99–109.
35. Curry MR, Redding BJ, Watson PF. Determination of water permeability coefficient and its activation energy for rabbit spermatozoa. *Cryobiology* 1995; 32:175–181.
36. Watson PF. Recent developments and concepts in the cryopreservation of spermatozoa and the assessment of their post-thawing function. *Reprod Fertil Dev* 1995; 7:871–891.
37. Noiles EE, Bailey JL, Storey BT. The temperature dependence in the hydraulic conductivity,  $L_p$ , of the mouse sperm plasma membrane shows a discontinuity between 4 and 0 °C. *Cryobiology* 1995; 32:220–238.
38. Gilmore JA, McGann LE, Liu J, Gao DY, Peter AT, Kleinhans FW, Critser JK. Effect of cryoprotectant solutes on water permeability of human spermatozoa. *Biol Reprod* 1995; 53:985–995.
39. Kleinhans FW, Travis VS, Du J, Villines PM, Colvin KE, Critser JK. Measurement of human sperm intracellular water volume by electron spin resonance. *J Androl* 1992; 13:498–506.
40. Wolkers WF, Balasubramanian SK, Ongstad EL, Zec HC, Bischof JC. Effects of freezing on membranes and proteins in LNCaP prostate tumor cells. *Biochim Biophys Acta* 2007; 1768:728–736.
41. Morris GJ. Rapidly cooled human sperm: no evidence of intracellular ice formation. *Hum Reprod* 2006; 21:2075–2083.
42. Hall JC, Hadley J, Doman T. Correlation between changes in rat sperm membrane lipids, protein, and the membrane physical state during epididymal maturation. *J Androl* 1991; 12:76–87.
43. Rejraji H, Sion B, Prensier G, Carreras M, Motta C, Frenoux JM, Vericel E, Grizard G, Vernet P, Drevet JR. Lipid remodeling of murine epididymosomes and spermatozoa during epididymal maturation. *Biol Reprod* 2006; 74:1104–1113.